International Journal of Scientific Engineering and Technology (ISSN : 2277-1581)
Volume No.3 Issue No.5, pp : 675-679 1 May 2014

Numerical Study on the Effect of Ratio among Various of Submersion on Three Dimensional Velocity Components around T-shaped Spur Dike Located in a 90 Degree Bend

M. Vaghefi[1*], M. Shakerdargah[2], M. Akbari[3]

[1,3]Department of Civil Engineering, Persian Gulf University, Bushehr, Iran.
[2]Department of Civil Engineering, Islamic Azad University, Bushehr, Iran
Corresponding Author Email: vaghefi@pgu.ac.ir

Abstract: ***Spur dike is one of the hydraulic structures used in rivers to protect river banks. In this paper, flow pattern around a T-shaped spur dike which is located in a 90◦ bend and different amounts of submersion has been studied using Flow-3D. Numerical results have been compared with experimental results and have been analysed.***

Keywords: **Submerged T-shaped Spur Dike, Three Dimensional Velocity, Flow Pattern, 90 Degree Bend, Flow-3D**

I. Introduction

Since long time ago, rivers have been considered one of the most basic sources of water for human civilization. Despite the vital role they play for human life, they have also been one of the natural enemies of human beings. Rivers have gone through changes in their life cycle, and erosion of outer walls and river beds, and sedimentation in inner walls are some instances which cause irreparable damage to inhabitants and constructions by the rivers.

Spur dikes are extended in rivers in a vertical or angular position in proportion to river walls. These structures protect river walls from erosion by redirecting the flow from the walls to the middle of the channel. Spur dikes change flow field, and cause a strongly turbulent three-dimensional flow. Horseshoe vortexes downstream the separation are formed because of a lot of pressure behind the structure, and the flow near the bed, and the flow down the upstream of the structure [i].

Gill in 1972, did an experimental study showing that the distance between the spur dikes is very much dependent on the radius of curvature [ii]. Rajaratnam & Nwachukwu studied the turbulent flow near groin in 1983. Based on experimental observations, the deflected flow has been analysed using the model of the three-dimensional turbulent boundary layer [iii]. Kong and Platfoot in 1996, investigated the effect of channel geometry and operational parameters on the flow pattern in a two dimensional model [iv]. Graf and Blanckaert in 2001, did an experimental study on a 120º bend channel and measured secondary flow and maximum velocity at the 60º cross section [v]. McCoy et al. in 2004, Investigated flow pattern around and between two spur dikes using LES method in an open channel [vi]. Fazli et al. in 2008, did an experimental study on a 90 degree bend channel to study the parameters affecting scour around straight spur dikes [vii]. Ghodsian and Vaghefi in 2009, carried out an experimental study on how changes in Froude Number, and length of wing and web of T-shaped spur dike affect flow pattern in a 90 degree bend [viii]. Duan in 2009, investigated average and turbulent flow around a straight spur dike located in an experimental channel with rigid bed [ix]. Since 2008, Vaghefi et al. have experimentally investigated flow pattern and scour around unsubmerged T-shaped spur dike in a 90 degree bend in different parameters including Froude number, curvature radius, spur dike position, spur dike geometry, time effect, flow conditions etc. [x-xii]. Acharya et al. in 2013, carried out a three-dimensional numerical investigation of turbulent flow pattern around series of straight spur dikes located in a straight route, using Flow-3D [xiii].

Since there has not been enough study on flow pattern around submerged spur dikes located in bend, in this study, the effect of submersion on flow pattern around T-shaped spur dike located in a 90 degree bend has been numerically investigated. Also, the results from numerical modelling have been compared with those from experimental model.

II. Material and Methodology

- Experimental Model Introduction

The intended experiments have been carried out by Vaghefi [x] in Hydraulics laboratory of Tarbiat Modares University in Iran, on a laboratory flume with the width of 60 cm, and the height of 70 cm, in a compound of straight and bend route. The straight upstream route is 710 cm long, and is connected to straight downstream route of 520 cm long via a 90 degree bend with an external radius of 270 cm, and an internal radius of 210 cm. The ratio of bend radius to width of channel is 4. Uniform sediments have an average diameter of 1.28 mm. Also the flow discharge equals to 25 lit/s. The spur dike used in this experiment is a T-shaped spur dike. The length of wing (L) and that of web (l) are equal to 9 cm, with the height of 25 cm. This spur dike is vertical and unsubmerged in a 45 degree position. The features of the laboratory flume and schematic view of the T-shaped spur dike is presented in Figure (1).

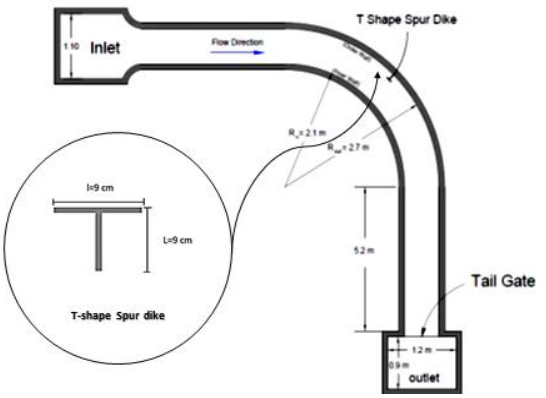

Figure (1): features of the laboratory flume and schematic view of T-shaped spur dike

International Journal of Scientific Engineering and Technology (ISSN : 2277-1581)
Volume No.3 Issue No.5, pp : 675-679 1 May 2014

- Numerical Model Introduction

FLOW-3D is one of the most powerful softwares concerning fluid dynamics which is developed and supported by Flow Science, Inc. It can do one- two- and three-dimensional analysis of flow field, and is very much useful in matters of fluids. Five different turbulence models are used in order to solve turbulent flows' features. The governing equations on fluid flow include Continuity equation and Momentum equation. Continuity equation in Cartesian coordinates (x,y,z) is as follows [xiv]:

$$V_F \frac{\partial(\rho)}{\partial t} + \frac{\partial}{\partial t}(uA_x) + \frac{\partial}{\partial y}(vA_y) + \frac{\partial}{\partial z}(wA_z) = \frac{R_{SOR}}{\rho} \quad (1)$$

Momentum equation for three-dimensional components of flow velocity is:

$$\frac{\partial u}{\partial t} + \frac{1}{V_F}\left(uA_x\frac{\partial u}{\partial x} + vA_y\frac{\partial u}{\partial y} + wA_z\frac{\partial u}{\partial z}\right) = -\frac{1}{\rho}\frac{\partial P}{\partial x} + G_x + f_x \quad (2)$$

$$\frac{\partial v}{\partial t} + \frac{1}{V_F}\left(uA_x\frac{\partial u}{\partial x} + vA_y\frac{\partial u}{\partial y} + wA_z\frac{\partial u}{\partial z}\right) = -\frac{1}{\rho}\frac{\partial P}{\partial y} + G_y + f_y \quad (3)$$

$$\frac{\partial w}{\partial t} + \frac{1}{V_F}\left(uA_x\frac{\partial u}{\partial x} + vA_y\frac{\partial u}{\partial y} + wA_z\frac{\partial u}{\partial z}\right) = -\frac{1}{\rho}\frac{\partial P}{\partial z} + G_z + f_z \quad (4)$$

In model analysis, explicit method along with RNG k-ε turbulence model has been utilized. In Figure (2), there is a view of the meshing produced in Flow 3D software.

- Verification

In order for the results of the numerical modelling to be verified, they are compared with the results of another experiment under the same conditions. In Figure (3), the experimental and numerical results pertaining to longitudinal, lateral, and vertical velocity components in cross section, and a distance of 0.25 times the length of upstream spur dike which is unsubmerged, and a Froude Number 0.34 are indicated. As is seen in Figure (3-a), away from the internal bend, longitudinal velocity increases, but close to the external bend, it decreases. Also, from the internal bend to the wing of the spur dike, velocieties are in the same direction and are the same amount, but from the wing of the spur dike to the external bend, velocity is in an opposite direction and decreases. In Figure (3-b), it is observed that away from the internal bend, lateral velocity increases, and the highest velocity is found near the wing of the spur dike. Also, from the wing of the spur dike to the external bend, the direction of velocity has changed. As is seen in Figure (3-c), the maximum vertical velocity is found in the middle of the channel, from the internal bend to the wing of the spur dike. Also, the most turbulence is observed between the wing of the spur dike and the external bend. According to these figures, the similarity of the results of Flow 3D software to those of the experiments indicates the verification of data analysis. This leads to verification of the results from numerical modelling.

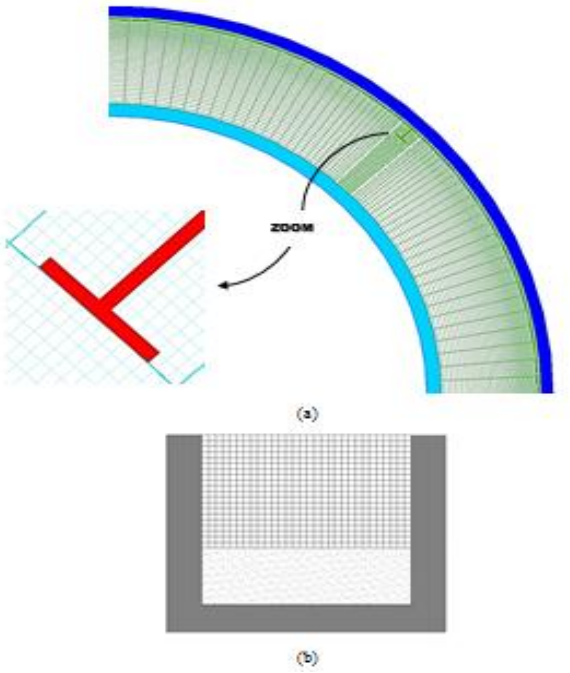

Figure (2): a view of the meshing produced by FLOW3D, a) on length and width; b) in depth

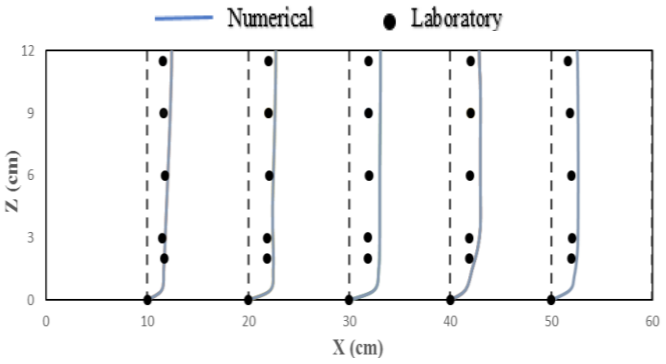

Figure (3-a): Verification of longitudinal velocity in cross section in a distance of 0.25 times the length of the upstream spur dike for Fr = 0.34 and with an unsubmerged spur dike, 20 cm/s

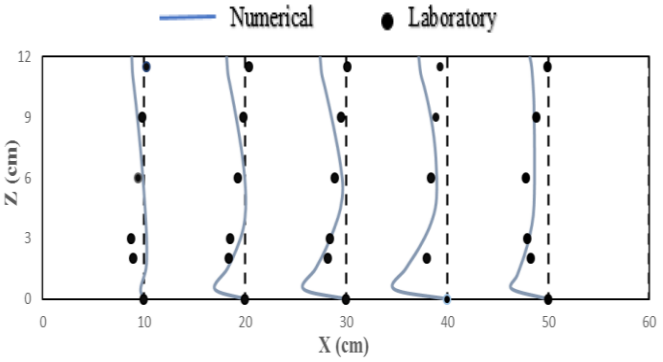

Figure (3-b): Verification of lateral velocity in cross section and in a distance of 0.25 times the length of the downstream spur dike for Fr= 0.34 and with an unsubmerged spur dike, 10 cm/s

International Journal of Scientific Engineering and Technology (ISSN : 2277-1581)
Volume No.3 Issue No.5, pp : 675-679 1 May 2014

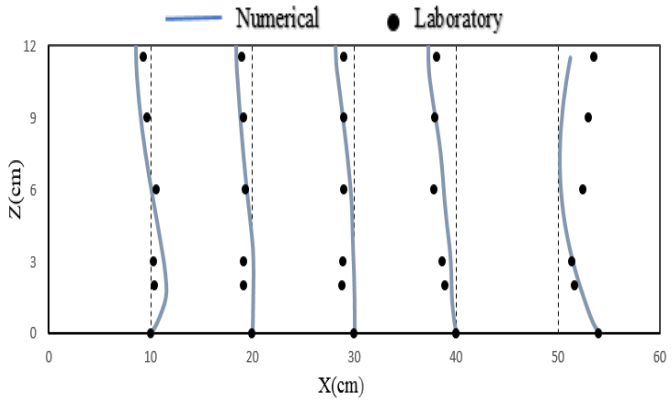

Figure (3-c): Verification of vertical velocity in cross section in a distance of 0.25 times the length of the downstream spur dike for Fr = 0.34 and with an unsubmerged spur dike, 2.5 cm/s

III. Results and Tables

- Study on flow pattern in cross section

In Figure 4, stream lines in cross section, and 0.25 times the length of the spur dike away upstream, with Froude Number 0.34 for different amounts of submersion are shown. In Figure (4-a), it is seen that stream lines are up flow and down flow. This flow leads to a clockwise vortex as big as 25% of the width of the channel, and an anticlockwise vortex as big as 17% of the width of the channel. Also, it is observed in Figures (4-b), and (4-c) that stream lines are moving toward the inner bend, and in a distance of 25% of the width of the channel from the inner wall they flow toward the middle of the channel, forming a clockwise vortex as big as 60% of the width of the channel. Also, another vortex is found which is as big as 17% of the width of the channel in an anticlockwise direction. As is seen in Figure (4-d), the flow behind the wing is up flow. The flow which is moving toward the inner bend from the surface, works as a return flow in a distance of 35% of the width of channel from the inner wall, and forms an anticlockwise vortex as big as 45% of the width of the channel. Also, in a distance of 25% of the width of the channel, a clockwise vortex as big as 60% of the width of the channel is seen. Finally, another vortex is formed on the surface of the channel which is as big as 30% of the width of the channel in an anticlockwise direction.

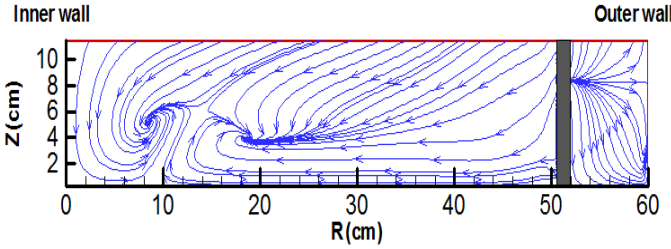

(a)

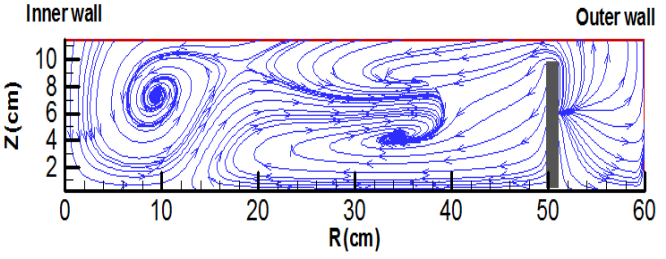

(b)

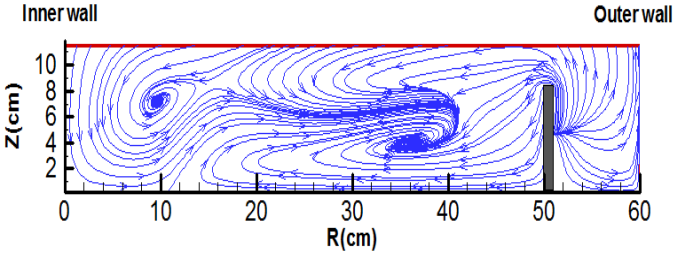

(c)

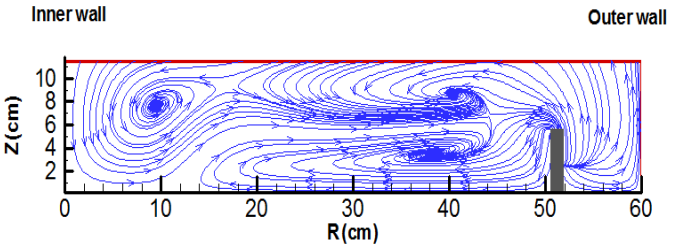

(d)

Figure (4): stream lines in cross section in a distance of 0.25 times the length of the spur dike upstream, with Froude Number 0.34, and spur dike submerged for a) 0% b) 15% c) 25% d) 50%

- Three-dimensional velocity components

In Figure (5), three-dimensional velocity components in a distance of 0.5 times the length of the spur dike upstream for Froude Number 0.34 are shown for different amounts of submersion. In Figure (5-a), it can be seen that closer to internal bend, with more submersion, longitudinal velocity decreases by half. In Figure (5-b), it is observed that near the internal bend, lateral velocities on surface and bed are in opposite directions, but away from the internal bend, lateral velocity on bed increases by about 60%. According to Figure (5-c), it is seen that away from the internal bend, vertical velocities in the middle and on the surface of the channel decrease by about 60%. When the submersion of the flow between the wing and the external bend increases, the flow is turbulent in an opposite direction.

- Study on flow pattern in longitudinal profile

In Figure (6), stream lines in cross section in a distance of 5% of the width of the channel from the external bend, with Froude Number 0.34, and different amounts of submersion are shown. In Figure (6-a), it can be seen that the flow forms a clockwise vortex near the bed upstream the spur dike. In Figures (6-b), (6-c), and (6-d), it is observed that upstream the spur dike and above the web, a vortex as big as 8% of the width of the channel is formed. As the spur dike is submerged more, there are fewer vortexes formed upstream. Also, as the spur dike is submerged more, vortexes are formed above the web and in a distance of 6% of the width of the channel.

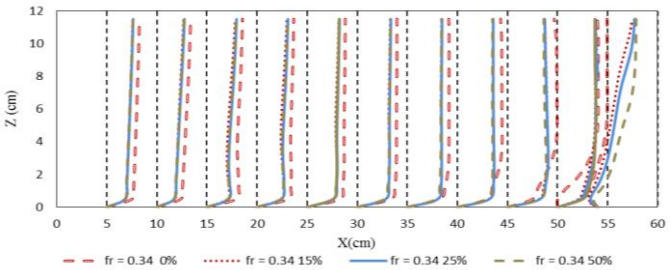

Figure (5- a): Lateral velocity components in a distance of 0. 5 times the length of the downstream spur dike for different amounts of submersion and Fr = 0.34, 20 cm/s

International Journal of Scientific Engineering and Technology (ISSN : 2277-1581)
Volume No.3 Issue No.5, pp : 675-679 1 May 2014

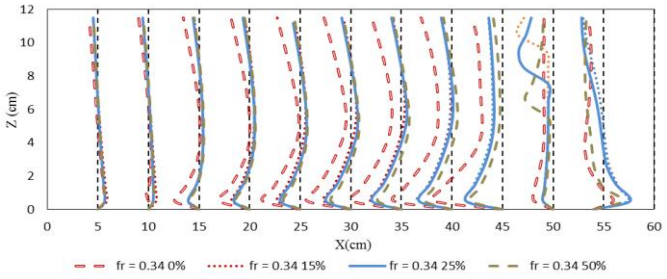

Figure (5- b): Longitudinal velocity components in a distance of 0. 5 times the length of the downstream spur dike for different amounts of submersion and Fr=0.34, 10 cm/s

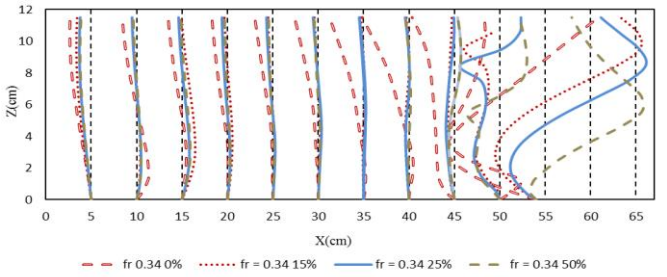

Figure (5- c): Vertical velocity components in a distance of 0. 5 times the length of the downstream spur dike for different amounts of submersion and Fr = 0.34, 2.5 cm/s

- flow pattern in plan

In Figure (7), stream lines in the plan near the bed, and around the spur dike are shown for Froude Number 0.34, and different amounts of submersion. In Figures (7-a), (7-b), and (7-c), it can be seen that the flow hits the spur dike and forms an anticlockwise vortex upstream, and after it hits the spur dike it changes direction and forms a vortex a lot larger than the previous one down the stream in an anticlockwise direction. Then, it flows toward the external bend. In Figure (7-d), it is seen that the flow moves straight after hitting the spur dike.

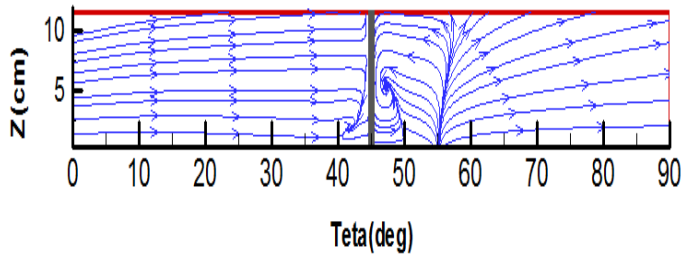

(a)

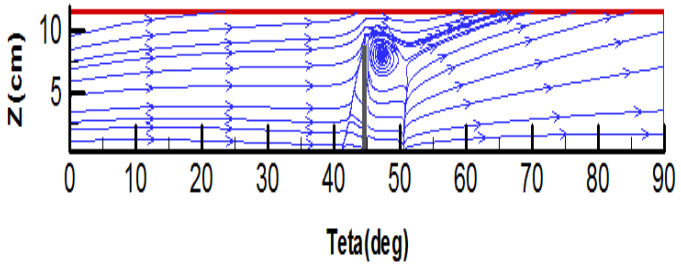

(b)

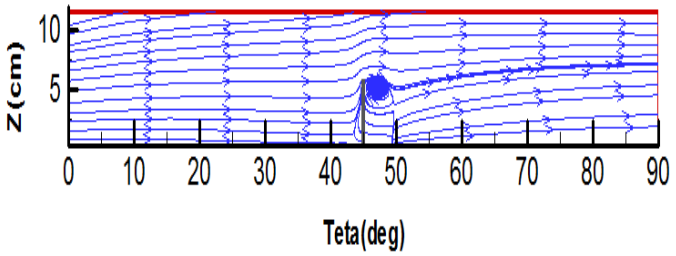

(c)

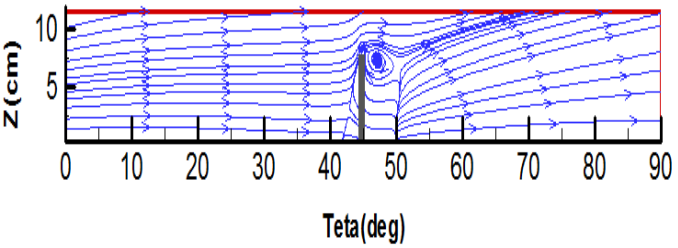

(d)

Figure (6): stream lines in longitudinal section in a distance of 5% of the width of the channel from the outer wall, Froude Number 0.34, and different amounts of submersion: a) 0% b) 15% c) 25% d) 50%

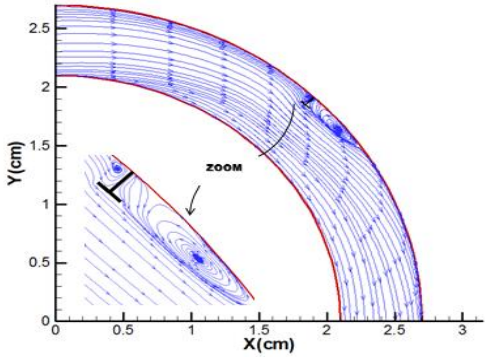

(a)

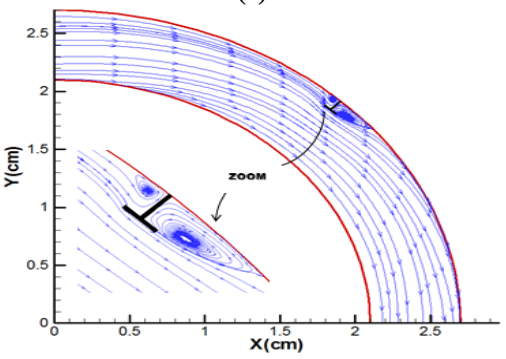

(b)

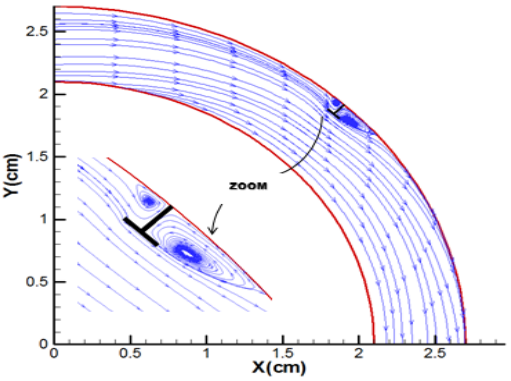

(c)

International Journal of Scientific Engineering and Technology (ISSN : 2277-1581)
Volume No.3 Issue No.5, pp : 675-679 1 May 2014

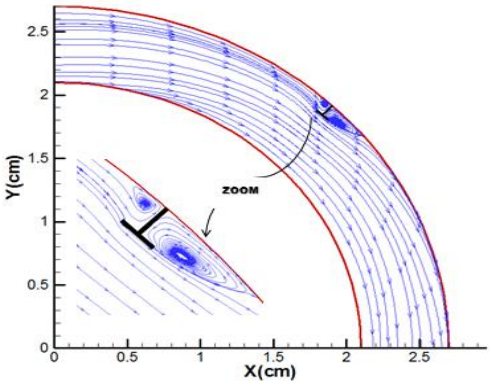

(d)

Figure (7): stream lines in a plan near the bed, with Froude Number 0.34, and different amounts of submersion: a) 0% b) 15% c) 25% d) 50%

IV. Conclusion

- With an increase in submersion of the spur dike, the flow changes into up flow behind the wing.
- Closer to internal bend, as the spur dike is submerged more, longitudinal velocity decreases by half.
- Away from the inner wall, lateral velocity on the bed of the channel increases by 60%.
- Away from internal bend, vertical velocities in the middle and on the surface decrease by about 60%.
- There is turbulent flow between the wing of the spur dike, and external bend, which changes direction when there is an increase in submersion.

References

i. Azinfar H. and Kells J.A., (2008). Backwater prediction due to the blockage caused by a single submerged spur dike in an open channel. Journal Hydraulic Engineering, Vol. 134, No. 8, pp. 1153–1157.

ii. Gill M.A., (1972). Erosion of Sand Beds around Spur dikes. Journal of Hydraulic Division, Vol. 98, No. 9, pp. 91-98.

iii. Rajaratnam N. and Nwachukwu B. A., (1983). Flow near groin-like structures. Journal of Hydraulic Engineering, Vol. 109, No. 3, pp. 463-480.

iv. Kong L.X. and Platfoot R., (1996). Two dimensional simulation of air flow in the transfer channel of open-end rotor spinning machines. Textile Research Journal, Vol.66, pp. 641-650.

v. Blanckaert K. and Graf W. H., (2001). Mean flow and turbulence in open-channel bend. Journal of Hydraulic Engineering, Vol. 127, No. 10, pp. 835-847.

vi. McCoy A., Constantinescu G. and Weber L., (2005). Coherent Structures in a Channel with Groyne Fields: A Numerical Investigation Using LES. Impacts of Global Climate Change, pp. 1-12.

vii. Fazli M., Ghodsian M. and Saleh Neyshabouri A.A., (2008). Scour and flow field around a spur dike in a 90° bend. Journal of Sediment Research, Vol. 23, No. 1, pp. 56-68.

viii. Ghodsian M. and Vaghefi M., (2009). Experimental study on scour and flow field in a scour hole around a T-shaped spur dike in a 90° bend. Journal of Sediment Research, Vol. 24, No. 2, pp. 145-158.

ix. Duan J., (2009). Mean flow and turbulence around a laboratory spur dike. Journal of Hydraulic Engineering, Vol. 135, No. 10, pp. 803-811.

x. Vaghefi M., Godsian M. and Salehi Neyshaboori S.A.A., (2009). Experimental Study on the Effect of a T-Shaped Spur Dike Length on Scour in a 90 degree channel bend. The Arabian Journal for Science and Engineering, Vol. 34, No. 2B.

xi. Vaghefi M., Ghodsian M. and Salehi Neyshabori S.A.A., (2012). Experimental Study on Scour around a T-Shaped Spur Dike in a Channel Bend. Journal of Hydraulic Engineering, Vol. 138, No.5, pp. 471-474.

xii. Vaghefi M., Ghodsian M. and Adib A., (2012). Experimental Study on the Effect of Froude Number on Temporal Variation of Scour around a T-shaped Spur Dike in a 90° Degree Bend. Applied Mechanics and Materials, Vol. 147, pp. 75-79.

xiii. Acharya A., Acharya A. and Duan J., (2013). Three Dimensional Simulation of Flow Field around Series of Spur Dikes. International Refereed Journal of Engineering and Science (IRJES), Vol. 2, No. 7, pp. 36-57.

xiv. Flow Science, Inc. (2008). FLOW-3D User's Manual. Flow Science, Inc., 9.3 editions.